

Adaptive Control for Multirotor Systems with Completely Uncertain Dynamics

Bingguo Mu, Ee Hwei Ng and Pakpong Chirattananon

Abstract—Thanks to their exceptional flying maneuverability and simple dynamics, multirotor systems have recently been developed and used for various applications. In low-cost prototypes or highly-customized systems; however, the uncertainties in model parameters may adversely affect the flight performance or lead to instability. In this paper, we proposed a Lyapunov-based adaptive flight controller capable of robustly stabilizing a multicopter with completely uncertain configurations and dynamics. We experimentally demonstrate that the controller is capable of stabilizing the vehicle with only crude knowledge of its rotor positions, mass distribution, moment of inertia, and aerodynamic coefficients. The results show that the attitude and altitude errors initially caused by the inaccurate system model significantly reduced after the activation of the adaptive scheme in real flights.

I. INTRODUCTION

Multirotor systems are mechanically simple, yet highly manoeuvrable, they can hover in place, land and takeoff vertically. These desirable qualities attract attention of scientists and engineers to conduct research on them in light of many potential applications such as in cinematography, agriculture, transportation, and geographical mappings [1]–[6]. The most popular and notable multirotor platform is a quadrotor, which has four rotors vertically aligned and fixed to a rigid airframe. These four rotors are usually placed in a square formation with equal distances to the center of mass (CM) of the whole vehicle. This symmetric configuration simplifies the calculation required for flight control and stabilization. For control, the quadrotor is commanded to adjust the rotational speed of each rotor by altering the electrical signals to the DC motors.

In most circumstances, the process of designing a flight controller for such multi-rotor systems rely on the prior knowledge of system properties such as the shape of a flying vehicle, the mass distribution and the aerodynamic coefficients of those propellers [7], [8]. In some situations, users or designers may not be able to obtain the reliable estimates of mentioned system parameters. This includes cases where a payload is attached to the vehicle or some components of vehicle are imprecisely manufactured (i.e. two similar propellers may exhibit vastly different aeromechanic properties). Some quantities, such as moment of inertia, are relatively difficult to measure or estimate accurately, particularly when the shape of the vehicle

is highly asymmetric (This leads to a non-diagonal inertia matrix). Fortunately, the modeling uncertainties can potentially be overcome by the implementation of adaptive methods in flight controller. On this topic, thus far, there have been several examples of the implementation of adaptive techniques in flight control of multirotor systems. For example, Dydek *et al.* proposed an adaptive controller for quadrotors when there is actuator failure or physical damage causing some loss-of-thrust [9]. For investigating the modeling uncertainty in a quadrotor, Lee *et al.* directly used computer-simulations to numerically compare the performance of a feedback linearization controller and that of an adaptive sliding mode controller [10]. Bouadi *et al.* studied a direct adaptive sliding mode control for the quadrotors, where a centered white gaussian noise are added to robotic parameters for testing the performance of handling uncertain aerodynamic parameters and modeling inaccuracies [11]. Most of these work, nevertheless, assume that only a few specific partial system parameters are uncertain.

In this paper, we investigate multirotors with almost completely uncertain system parameters including the entire shape of the vehicle. Specifically, we want to eliminate the need to have a prior knowledge of exact rotor configuration, moment of inertia, and propeller coefficients. In this study, we do not directly use the relative distance between each rotor and the CM of vehicle, alternatively we only rely on their reasonable estimates. Starting from the estimated relative distances, we can further have an initial estimate of its moment of inertia and then formulate an initial dynamic matrix describing the flight dynamics of the whole vehicle. Since this matrix is an approximated one, an adaptive control method with a proven Lyapunov stability is then implemented to enhance the flight performance for hovering flights. For simplicity, a customized quadrotor prototype is implemented only to verify the proposed adaptive flight controller in this paper. This should not affect the potential applications of the proposed flight controller on other multirotor systems. Furthermore, the proposed control algorithms in this paper are relatively simple, efficient and, therefore, can be easily implemented.

This paper will contribute to the field of micro aerial vehicles by addressing the issues arising from the use of imperfect prototypes and customized designs. The proposed adaptive method will allow developers to rapidly and robustly design a flight controller for highly customized systems or improve the flight performance of an existing vehicle with an added payload.

This work was supported by the Research Grants Council of the Hong Kong Special Administrative Region of China (grant number CityU-11274016).

The authors are with the Robotics and Intelligent Systems Laboratory, Department of Mechanical and Biomedical Engineering, City University of Hong Kong, Hong Kong SAR, China (email: bingguomu2-c@my.cityu.edu.hk, pakpong.c@cityu.edu.hk).

II. DYNAMIC MODELING

In this part, dynamic model of a multirotor vehicle with uncertain parameters will be outlined, together with a proposed estimation strategy.

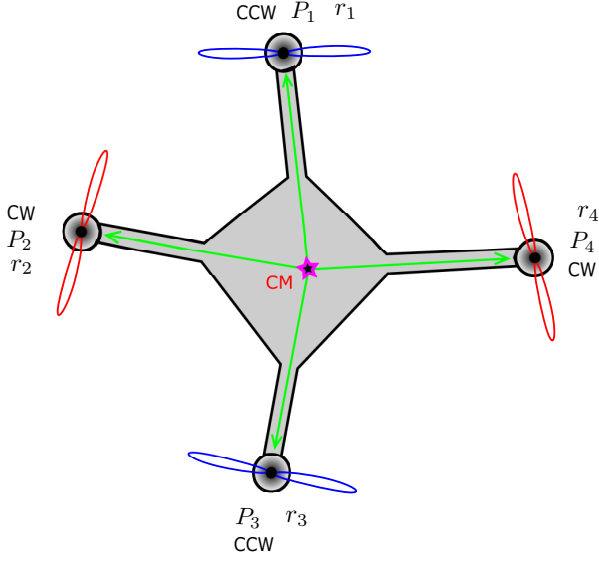


Fig. 1. Concept of a multirotor vehicle with completely uncertain dynamics, where r_i denotes the relative distance between the i^{th} rotor and the CM of the whole vehicle and P_i denotes the position of each rotor in inertial frame.

A. Coordinate Frames

There are two reference frames required for describing the flight dynamics. The first coordinate system is fixed and called the Earth frame or inertial frame. The second reference frame translates and rotates with the aircraft at the center of mass, called the body frame. In this paper, symbols ϕ , θ and ψ (or roll, pitch and yaw angles) are used to denote Euler angles representing the rotation about the x-axis, y-axis and z-axis of the multirotor system [12], [13]. The symbol $\omega = [\omega_x, \omega_y, \omega_z]^T$ denotes the angular velocity in the body frame which is generally different from the time-derivative of the Euler angles or $[\dot{\phi}, \dot{\theta}, \dot{\psi}]^T$.

B. Dynamic Model of Multirotor Vehicle

Fig. 1 illustrates a schematic diagram of a quadrotor. Based on the blade-element method [1], each spinning propeller approximately produces a thrust force $T_i = k\Omega_i^2$ and induces a drag torque $\tau_{di} = b\Omega_i^2$ (along the z-axis). Here, Ω is the angular velocity of the propeller, k and b are thrust and torque constants to be experimentally determined or calculated via the blade element method [14]. In order to control and stabilize the vehicle, various system parameters, such as the center of mass (CM), the moment of inertia and rotor's k and b must be known [11]. The location of each rotor with respect to the CM dictates the amount of torque the rotor contributes to the dynamics of the vehicle. In this paper, we define the relative distance r_i as a vector originating from the CM location to the i^{th} rotor. Combining r_i with other dynamic-related information such as the spinning direction of each rotor, thrust constant k

and torque constant b , we can determine the total thrust force T , and the total torque $\tau = [\tau_\phi, \tau_\theta, \tau_\psi]^T$ generated in terms of Ω by a dynamic matrix as:

$$\begin{bmatrix} T \\ \tau_\phi \\ \tau_\theta \\ \tau_\psi \end{bmatrix} = A'u = A' \begin{bmatrix} \Omega_1^2 \\ \vdots \\ \Omega_N^2 \end{bmatrix}, \quad (1)$$

where $A' \in R^{4 \times N}$ is the so-called dynamic matrix. The control input is defined as $u = [\Omega_1^2, \dots, \Omega_N^2]^T \in R^{N \times 1}$ with N denoting the number of rotors. In typical circumstances, these r_i are precisely known in advance and the rotors are symmetrically arranged. In this research, we consider the case where only the uncertain estimates of these r_i are available. If $r_i := [r_{i,x}, r_{i,y}]^T$ can be accurately estimated, the dynamic matrix in (1) can be explicitly written as:

$$A' = \begin{bmatrix} k & \cdot & \cdot & k \\ kr_{1,y} & \cdot & \cdot & kr_{N,y} \\ -kr_{1,x} & \cdot & \cdot & -kr_{N,x} \\ (-1)^{c_1}b & \cdot & \cdot & (-1)^{c_N}b \end{bmatrix}, \quad (2)$$

where the auxiliary coefficient symbol c_i denotes the i^{th} rotor's spinning direction (when the rotor spins counter-clockwise or CCW, $c_i := 1$, and $c_i := 0$ when the i^{th} rotor spins clockwise or CW) with index $i = 1, \dots, N$.

C. Estimation of the Moment of Inertia

Treating the vehicle as a rigid body, its rotational dynamics follow the Euler's rotation equation: $\tau = I\dot{\omega} + \omega \times I\omega$ where " $\omega \times I\omega$ " $\rightarrow 0$ when ω is small (near hovering condition). In this paper, we limit our analysis for hovering flight (ω is small). In fact, the configuration of the investigated multirotor is asymmetric, which results in a non-diagonal inertia matrix I . For simplicity, the initial estimate of the inertial matrix I is assumed to be a diagonal matrix $\text{diag}[I_{xx}, I_{yy}, I_{zz}]$. This diagonal assumption is solely for the estimation purpose as the proposed adaptive control scheme in Section III does not require this simplification. In this situation, the force and torques can be simplified as $T \approx m(\ddot{z} + g)$, $\tau_\phi \approx I_{xx}\dot{\omega}_x$, $\tau_\theta \approx I_{yy}\dot{\omega}_y$ and $\tau_\psi \approx I_{zz}\dot{\omega}_z$. Thus the dynamic model (1) can be rewritten as:

$$\begin{bmatrix} \ddot{z} + g \\ \dot{\omega}_x \\ \dot{\omega}_y \\ \dot{\omega}_z \end{bmatrix} = \begin{bmatrix} m & 0 & 0 & 0 \\ 0 & I_{xx} & 0 & 0 \\ 0 & 0 & I_{yy} & 0 \\ 0 & 0 & 0 & I_{zz} \end{bmatrix}^{-1} A'u \quad (3)$$

$$= Au = A[\Omega_1^2, \dots, \Omega_n^2]^T,$$

where we have defined the dynamic matrix A that takes into account the moment of inertia. If the mass of the i^{th} rotor component (including ESC, propeller, etc.) is denoted as m_i , then we can approximately estimate the moment of inertia of the vehicle in each diagonal element as $I = \sum_{i=1}^N [m_i(r_i)^2]$. In addition to the mass from each rotor, there are other auxiliary mechanical parts including chassis and onboard controller on such multirotor vehicle where the new inertial matrix (denoted as I') needs to be known or estimated. In this paper, we directly estimate it based on r_i to simplify the whole formulation. If the

mass of such auxiliary mechanical part is estimated as γm_i , where $\gamma > 0$ is an estimated scalar constant, thus the mass of a whole flying vehicle satisfies $m = (N + \gamma)m_i$. Since the CM of such unknown auxiliary mechanical part is likely inside the convex hull of an object consisting of all rotors, which means it is relatively closer to the CM of the whole flying vehicle. We can approximate $I' \approx \sum_{i=1}^N [m_i(r_i)^2]$ with $m_i \approx \frac{m}{N + \gamma}$.

With considering the studied moment of inertia I' with $I'_{xx} \approx \frac{m}{N + \gamma} \sum_{i=1}^N (r'_{i,y})^2$, $I'_{yy} \approx \frac{m}{N + \gamma} \sum_{i=1}^N (r'_{i,x})^2$ and $I'_{zz} = I'_{xx} + I'_{yy}$, the matrix A in (3) can be rewritten as:

$$\begin{bmatrix} \frac{k}{m} & \dots & \frac{k}{m} \\ \frac{(N + \gamma)kr_{1,y}}{m \sum_{i=1}^N (r_{i,y})^2} & \dots & \frac{(N + \gamma)kr_{N,y}}{m \sum_{i=1}^N (r_{i,y})^2} \\ -\frac{(N + \gamma)kr_{1,x}}{m \sum_{i=1}^N (r_{i,x})^2} & \dots & -\frac{(N + \gamma)kr_{N,x}}{m \sum_{i=1}^N (r_{i,x})^2} \\ \frac{(N + \gamma)(-1)^{c_1} b}{m \sum_{i=1}^N [(r_{i,x})^2 + (r_{i,y})^2]} & \dots & \frac{(N + \gamma)(-1)^{c_N} b}{m \sum_{i=1}^N [(r_{i,x})^2 + (r_{i,y})^2]} \end{bmatrix} \cdot (4)$$

III. CONTROLLER DESIGN

In contrast to the conventional approach, e.g., Mahony and Corke [5] where the configuration of the vehicles and the dynamics of each rotor are pre-identified and precisely known, our focus in this paper is to stabilize a multirotor vehicle with completely uncertain dynamics. These rotors may be asymmetrically arranged on a horizontal plane but they should vertically align. The asymmetric configuration renders it difficult to evaluate the center of mass and the moment of inertia. It follows that r_i 's are not precisely known. Besides, in our case, aerodynamic parameters, such as thrust and torque constants (k , b), are only approximately known. Thus it is challenging to obtain the dynamic matrix in (4). This makes it increasingly difficult to achieve robust and accurate control of the vehicle. In this section, the Lyapunov-based adaptive control method is proposed to stabilize the flying vehicle in hovering flights. Fig. 2 shows the block diagram of the proposed control. The lateral controller is cascaded with the adaptive controller, which includes the attitude controller and the altitude (z) controller. Our focus is the adaptive controller. The lateral controller is only for keeping the vehicle in the designated area. Notice that, onboard IMU sensor can provide the realtime orientation information for attitude controller and the realtime position information is provided by motion capture system (MOCAP).

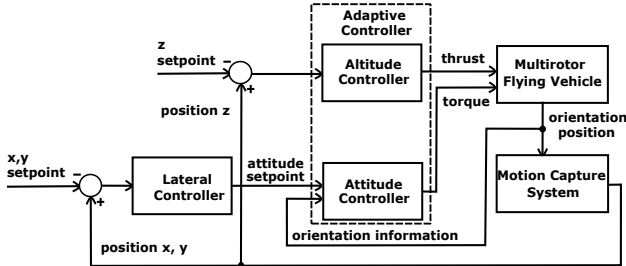


Fig. 2. Block diagram showing the overall structure of the controller.

A. Adaptive Control Strategy

Since there are many parameters that are not precisely estimated, the adaptive control method is used for designing

the control law of input u . Assuming the thrust vector of all rotor are aligned with the z-axis of the body frame, we obtain the following by combining equations (3) and (4):

$$\begin{bmatrix} \ddot{z} \\ \dot{\omega}_x \\ \dot{\omega}_y \\ \dot{\omega}_z \end{bmatrix} + \begin{bmatrix} g \\ 0 \\ 0 \\ 0 \end{bmatrix} = \ddot{\beta} + \vec{g} = A \begin{bmatrix} \Omega_1^2 \\ \cdot \\ \cdot \\ \Omega_n^2 \end{bmatrix} = Au, \quad (5)$$

where symbols $\ddot{\beta} = [\ddot{z}, \dot{\omega}_x, \dot{\omega}_y, \dot{\omega}_z]^T$ (or $\beta = [z, \phi, \theta, \psi]^T$), $\vec{g} = [g, 0, 0, 0]^T$. Note that the dynamic matrix A is simply a product of the inverse of the inertia matrix and A' , which does not require the inertia matrix to be diagonal. Based on the adaptive control theory [15], the control and adaptation law can be designed as:

$$\begin{aligned} u &= (\hat{A})^{-1}(\ddot{\beta}_d - 2K\dot{\tilde{\beta}} - K^2\tilde{\beta} + \vec{g}), \\ \dot{\hat{A}} &= \Lambda s u^T, \end{aligned} \quad (6)$$

where \hat{A} is the estimate of A , $\tilde{\beta} = \beta - \beta_d$ represents the error of the current dynamics from the desired value β_d , slide mode parameter $s = \dot{\tilde{\beta}} + K\tilde{\beta}$ is a quantity that quantifies the errors in flight attitude and flight altitude we wish to minimize, $K = \text{diag}[k_z, k_{a\phi}, k_{a\theta}, k_{a\psi}]$ is a positive-definite gain diagonal matrix for the adaptive controller, and the positive-definite diagonal matrix $\Lambda = \text{diag}[\lambda_z, \lambda_{a\phi}, \lambda_{a\theta}, \lambda_{a\psi}]$ is for adjusting adaptive control rate.

Proof. If the dynamic matrix A is square (which means there are only four rotors), then we define control law $u = \hat{B}(\ddot{\beta} + \vec{g})$ where the real value of A satisfy $A = B^{-1}$, its estimate \hat{A} satisfies $\hat{A} = A + \tilde{A}$, $\dot{\hat{A}} = \dot{A} + \dot{\tilde{A}}$, $\hat{B} = B + \tilde{B}$ and $\dot{\hat{B}} = \dot{B} + \dot{\tilde{B}}$. The target is to make the slide mode parameter s (i.e., $\dot{\tilde{\beta}}, \tilde{\beta}$) converges to zero, and the corresponding Lyapunov function and its time-derivative term are chosen as:

$$\begin{aligned} V &= \frac{1}{2} s^T s + \frac{1}{2} \Lambda^{-1} \text{trace}(\tilde{A}^T \tilde{A}), \\ \dot{V} &= s^T \dot{s} + \Lambda^{-1} \text{trace}(\dot{\tilde{A}}^T \tilde{A}) \\ &= s^T [\dot{\tilde{\beta}} + K\dot{\tilde{\beta}}] + \Lambda^{-1} \text{trace}(\dot{\tilde{A}}^T \tilde{A}) \\ &= s^T [-Ks + \ddot{\tilde{\beta}} + K\dot{\tilde{\beta}} + Ks] + \Lambda^{-1} \text{trace}(\dot{\tilde{A}}^T \tilde{A}) \\ &= -s^T Ks + s^T (\hat{A}\hat{B} - I)(\ddot{\beta}_d - 2K\dot{\tilde{\beta}} - K^2\tilde{\beta} + \vec{g}) \\ &\quad - s^T \tilde{A}u + \Lambda^{-1} \text{trace}(\dot{\tilde{A}}^T \tilde{A}). \end{aligned}$$

where " $\hat{A}\hat{B} = I$ " and " $\Lambda^{-1} \text{trace}(\dot{\tilde{A}}^T \tilde{A}) = s^T \tilde{A}u$ " are chosen to hold for the purpose of satisfying the condition $V \geq 0$, $\dot{V} = -s^T Ks \leq 0$, and thus $\dot{\hat{A}} = \dot{A} + \dot{\tilde{A}} = \Lambda s u^T$. Note that, when $\dot{V} \rightarrow 0$, we have $s \rightarrow 0$ and resulting $\dot{\hat{A}}$ becoming zero regardless whether $\hat{A} \rightarrow A$ or not. This means that the above adaptive control can always minimize the sliding mode parameter s , but it does not guarantee that $\hat{A} \rightarrow A$. Finally, we obtain the following:

$$\begin{aligned} u &= (\hat{A})^{-1}(\ddot{\beta} + \vec{g}), \\ \dot{\hat{A}} &= \Lambda s u^T, \\ \ddot{\beta} &= \ddot{\beta}_d - 2K\dot{\tilde{\beta}} - K^2\tilde{\beta}. \end{aligned}$$

If $A \in R^{4 \times N}$ is not a square matrix (the number of rotors of multirotor $N > 4$), $u = \hat{A}^T(\hat{A}\hat{A}^T)^{-1}(\hat{\beta} + \hat{g})$ is substituted with $u \in R^{N \times 1}$ and the proof remains valid. ■

B. Underlying Principle of the Proposed Control Strategy

To better understand the proposed controller, we look at the scenario where the matrix A is precisely known ($\hat{A} = A$). Assuming no other disturbances in flight, the substitution of the control law in equation (6) to the dynamic equation (5) will result in the following equations:

$$\begin{cases} \ddot{z} = T/m - g = \ddot{z}_d - 2k_z(\dot{z} - \dot{z}_d) - k_z^2(z - z_d), \\ \ddot{\phi} = \dot{\omega}_x = \ddot{\phi}_d - 2k_{a\phi}(\dot{\phi} - \dot{\phi}_d) - k_{a\phi}^2(\phi - \phi_d), \\ \ddot{\theta} = \dot{\omega}_y = \ddot{\theta}_d - 2k_{a\theta}(\dot{\theta} - \dot{\theta}_d) - k_{a\theta}^2(\theta - \theta_d), \\ \ddot{\psi} = \dot{\omega}_z = \ddot{\psi}_d - 2k_{a\psi}(\dot{\psi} - \dot{\psi}_d) - k_{a\psi}^2(\psi - \psi_d), \end{cases} \quad (7)$$

where k_z , $k_{a\phi}$, $k_{a\theta}$ and $k_{a\psi}$ may be different with each other but all of them are positive scalar number. From equation (7), it can be seen that altitude and attitude of the robot will converge to their respective setpoints. Nevertheless this is no longer guaranteed when matrix A is unknown ($\hat{A} \neq A$).

C. Lateral Controller

The purpose of the lateral controller is to calculate the desired attitude setpoint (roll angle ϕ , pitch angle θ) based on current obtained position information in order to ensure that the vehicle stays in the flight arena during the experiment. These angles will be supplied as setpoints for the adaptive/attitude controller presented earlier. Generally, the lateral control law in this paper is formulated based on:

$$\begin{aligned} \begin{bmatrix} \ddot{x} \\ \ddot{y} \end{bmatrix} &= \frac{T}{m} \begin{bmatrix} \sin(\theta) \\ -\sin(\phi) \cos(\theta) \end{bmatrix} \\ &= \begin{bmatrix} \ddot{x}_d - k_d^{xy}(\dot{x} - \dot{x}_d) - k_p^{xy}(x - x_d) \\ \ddot{y}_d - k_d^{xy}(\dot{y} - \dot{y}_d) - k_p^{xy}(y - y_d) \end{bmatrix}, \end{aligned}$$

where k_d^{xy} , k_p^{xy} are positive gain values, $[x_d, y_d]^T$ is the position setpoint. Ideally, the desired roll angle ϕ_d and pitch angle θ_d can be calculated based on the thrust T and \ddot{x} , \ddot{y} . In hovering flight ($T \approx mg$), the desired angles are simply calculated as: $\phi_d \approx [k_d^{xy}\dot{y} + k_p^{xy}(y - y_d)]/g$ and $\theta_d \approx [-k_d^{xy}\dot{x} - k_p^{xy}(x - x_d)]/g$. Note that, the value of k_p^{xy} , k_d^{xy} should be smaller than the value of $k_{a\phi}$, $k_{a\theta}$ and $k_{a\psi}$ due to the fact that the attitude controller should convergent faster to the desired orientation (attitude setpoint at each instant of time) which is provided by the lateral controller.

IV. EXPERIMENTS

A quadrotor prototype with an asymmetric configuration is used to validate the proposed control strategy in this section.

A. Experimental Setup

Fig. 3 shows the flight arena. A ground-based computer receives the realtime vehicle position information from the MOCAP system (OptiTrack), and then wirelessly transmits it to the flying vehicle.

The lateral controller and the adaptive controller were implemented on a Pixhawk autopilot flight controller hardware which is an industrial standard microcontroller that

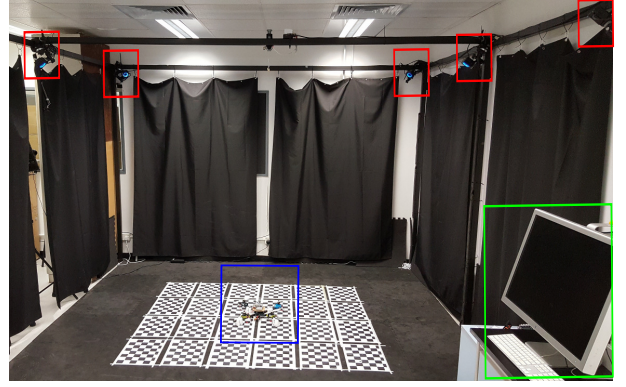


Fig. 3. General diagram shows indoor flight arena, where ground computer (in green square) provides position information (captured the MOCAP system in red squares) and receives debug information wirelessly to and from the flying vehicle (in blue square) respectively.

allows users to generate targeted binary codes based on Matlab/Simulink models [16]. Command and debug information between Pixhawk and ground computer are wirelessly transmitted by using the UDP and serial communication protocols.

The multirotor system is a quadrotor flying vehicle shown in Fig. 4, where the rotors M1 and M2 rotate in the CW direction and rotors M3 and M4 rotate in the CCW direction. The IMU module of Pixhawk autopilot can provide the real-time orientation and angular velocity measurements of this vehicle for the proposed attitude controller. However, since the measurement of yaw angle ψ is inaccurate in indoor environments, we opt to directly integrate the yaw rate $\dot{\psi}$ to estimate the yaw angle or heading of the robot.

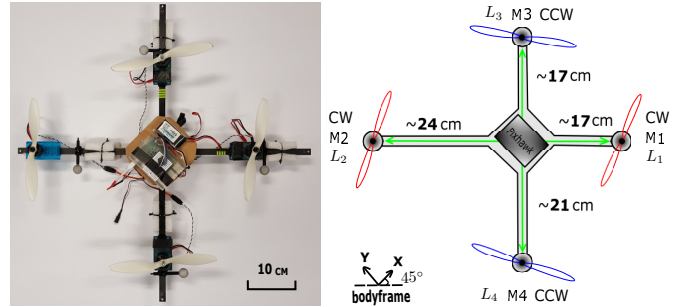


Fig. 4. A quadrotor prototype with its body frame defined, where L_i denotes the linkage between the i^{th} rotor and Pixhawk autopilot.

B. Hovering Flights Experiments

In our multirotor prototype, we do not know vehicle's exact CM location and its moment of inertia, hence, we need to estimate those $r_i = [r_{i,x}, r_{i,y}]$ firstly and then use them to approximate the vehicle's moment of inertia (the initial estimate assumes I to be diagonal). In our experiments, the initial CM of the whole vehicle is assumed to be located underneath the Pixhawk autopilot. For simplicity, the initial value of $\|r_i\|_2$ is assumed to be the length of linkage L_i as shown in Fig. 4. Based on visual observations, we estimate the initial lengths of L_i as $L_1 = \|r_1\|_2 = 0.18$ m, $L_2 = \|r_2\|_2 = 0.18$ m,

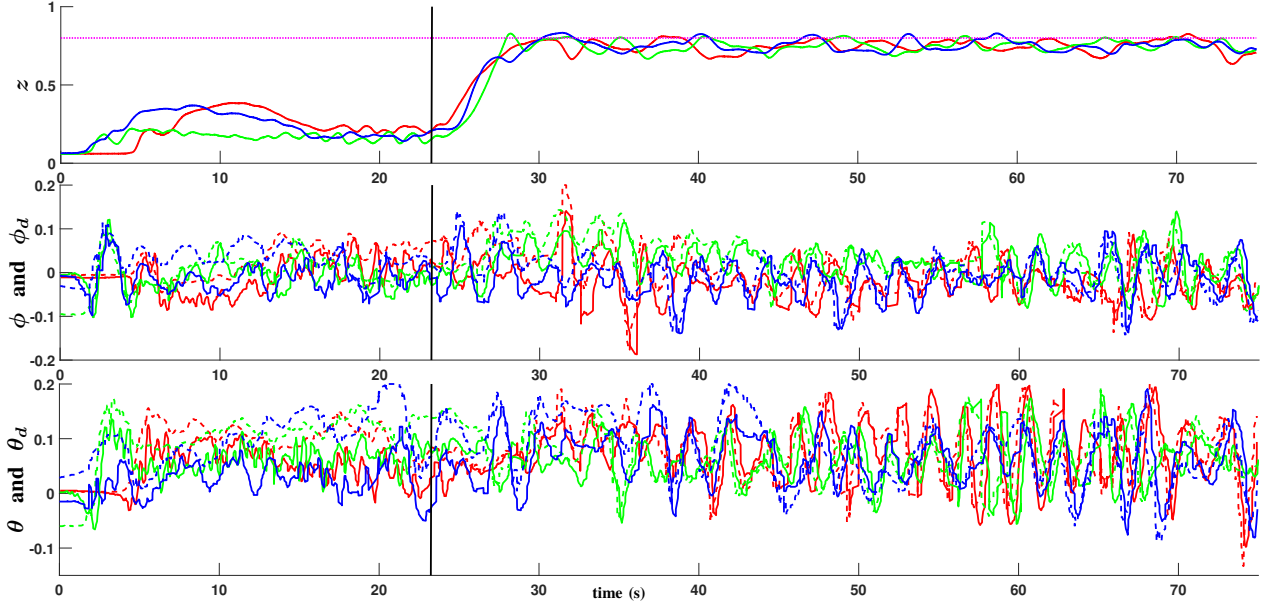


Fig. 6. Realtime observations of z , ϕ and θ in three experiments denoted by three different colors during a 75s long hovering flight, where the back solid lines are used to indicate the time when the adaptive control is activated. In addition, the magenta dotted line in the upper subplot denotes the desired altitude setpoint and colorful dashed lines in other subplots denote the desired real-time attitude setpoints ϕ_d and θ_d provided from the lateral controller.

$L_3 = \|r_3\|_2 = 0.18$ m and $L_4 = \|r_4\|_2 = 0.18$ m (the actual length ranges from ~ 0.17 to ~ 0.24 m via measurement). With this estimation, the proposed controller will initially command the rotors to generate the identical thrust. In our prototype ($m = 1.07$ kg), the auxiliary mechanical part's mass can not be ignored and we estimate $\gamma = 2$. Thus we can get an initial dynamic matrix \hat{A} which inevitably deviates from the actual A . Due to limited space in our indoor flight environment (the maximum height is 2 m), we used the RC remote to assist the altitude controller by providing the feedforward term to overcome the gravity.

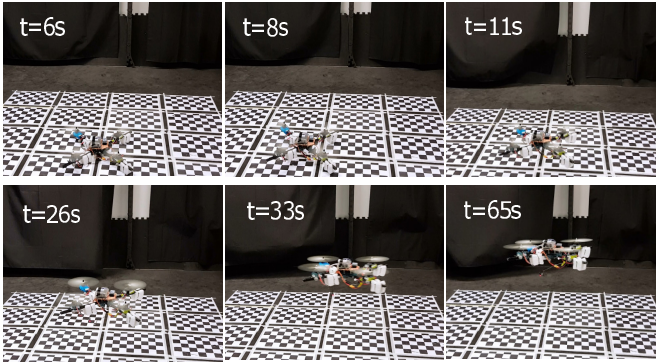


Fig. 5. Images of the real quadrotor prototype during a hovering flight.

We performed three hovering flights with the proposed adaptive controller. Each flight duration lasts over 60 seconds. For comparison, the adaptive scheme was only activated in the later portions of the flights. Note that, the lateral controller in our experiments is only implemented to provide attitude setpoints to prevent the vehicle escaping the flight area, thus we only present the experimental results related to the attitude

and altitude of the vehicle. Fig. 5 illustrates several images of the real quadrotor prototype for a hovering flight. The detailed results are illustrated in Figs. 6, 7 and 8.

Fig. 6 illustrates the realtime altitude position and orientation information during a 75-second long hovering flight. The top plot shows that in all three flights, the robot failed to reach the desired altitude setpoint $z_d = 0.8$ m before the adaptive control scheme was enabled (prior to the black solid boundary line). Once enabling the adaptive control, the matrix \hat{A} was adaptively updated at a frequency of 50 Hz, The adaptive scheme effectively adjusted the estimate of matrix A to reflect the inaccuracy in the thrust coefficient k , resulting in the vehicle quickly reaching the desired altitude. In other subplots, it can be seen that, without the adaptive scheme, the attitude of the vehicle failed to converge to the desired attitude setpoint ϕ_d and θ_d as well. However, the attitude tracking performance radically improved after the adaptive scheme was activated. Similarly, the reason is that the adaptive control scheme can gradually updated matrix \hat{A} such that the tracking errors in attitude and altitude are minimized.

To further demonstrate the results, Fig. 7 shows us the real-time error observations of four elements in $\tilde{\beta} = [\tilde{z}, \tilde{\phi}, \tilde{\theta}, \tilde{\psi}]^T$. In the top plot, the error in altitude $\tilde{z} = z - z_d$ converges to zero after enabling the adaptive component. In the remaining three subplots, attitude controller before enabling adaptive control can not fully control the orientation angles where we see all angular errors $\tilde{\phi} = \phi - \phi_d$, $\tilde{\theta} = \theta - \theta_d$ and $\tilde{\psi} = \psi - \psi_d$ are almost always either positive or negative in the first 23 seconds, especially the yaw angle. Once the adaptive control is enabled, these angular errors start to converge to zero. In fact, these CW spinning and CCW propellers in our quadrotor prototype turned out to have vastly different physical profiles

V. DISCUSSION AND CONCLUSION

In this paper, we investigated multirotor systems with completely uncertain dynamics, such as unknown mass distribution, moment of inertia, rotor configuration, imprecise relative distance estimates and aerodynamic constants. We first estimated the center of mass position to approximate the mass distribution of vehicle. Then, the vehicle's moment of inertia was estimated based on relative distance between the rotors and the CM. Thus we proposed a matrix which can feature the dynamics of the vehicle. Lastly, the lateral, altitude and attitude controller based on an adaptive control method was formulated and implemented. Experimental results of hovering flights on a quadrotor prototype verified the effectiveness of the proposed control scheme. In future multirotor systems, we will develop new algorithms for estimating the relative distances. One potential solution is to assign each rotor with an IMU, then to develop a data-fusing algorithm for extracting the relative distance among those rotors based on multiple IMU readings. Furthermore, multirotor prototypes with more than four rotors will be developed in future for verifying our proposed adaptive control strategy as well.

REFERENCES

- [1] *Pilot's Handbook of Aeronautical Knowledge*, ser. FAA-H-8083-25B. Oklahoma City, USA: Federal Aviation Administration (FAA), 2016.
- [2] B. Siciliano and O. Khatib, *Springer handbook of robotics*. Springer, 2016.
- [3] K. Y. Ma, P. Chirattananon, S. B. Fuller, and R. J. Wood, "Controlled flight of a biologically inspired, insect-scale robot," *Science*, vol. 340, no. 6132, pp. 603–607, 2013.
- [4] D. Floreano and R. J. Wood, "Science, technology and the future of small autonomous drones," *Nature*, vol. 521, no. 7553, p. 460, 2015.
- [5] V. K. R. Mahony and P. Corke, "Multirotor aerial vehicles modeling, estimation, and control of quadrotor," *IEEE Robotics & Automation Magazine*, vol. 19, no. 3, pp. 20–32, 2012.
- [6] T. Du, A. Schulz, B. Zhu, B. Bickel, and W. Matusik, "Computational multicopter design," *ACM Transaction on Graphics*, 2016.
- [7] K. Sreenath, N. Michael, and V. Kumar, "Trajectory generation and control of a quadrotor with a cable-suspended load—a differentially-flat hybrid system," in *Robotics and Automation (ICRA), 2013 IEEE International Conference on*. IEEE, 2013, pp. 4888–4895.
- [8] K. Sreenath and V. Kumar, "Dynamics control and planning for cooperative manipulation of payloads suspended by cables from multiple quadrotor robots," *m*, vol. 1, no. r2, p. r3.
- [9] Z. T. Dydek, A. M. Annaswamy, and E. Lavretsky, "Adaptive control of quadrotor uavs: A design trade study with flight evaluations," *IEEE Transactions on control systems technology*, vol. 21, no. 4, pp. 1400–1406, 2013.
- [10] D. Lee, H. J. Kim, and S. Sastry, "Feedback linearization vs. adaptive sliding mode control for a quadrotor helicopter," *International Journal of control, Automation and systems*, vol. 7, no. 3, pp. 419–428, 2009.
- [11] H. Bouadi, S. S. Cunha, A. Drouin, and F. Mora-Camino, "Adaptive sliding mode control for quadrotor attitude stabilization and altitude tracking," in *Computational Intelligence and Informatics (CINTI), 2011 IEEE 12th International Symposium on*. IEEE, 2011, pp. 449–455.
- [12] J. Diebel, "Representing attitude: Euler angles, unit quaternions, and rotation vectors," *Matrix*, vol. 58, no. 15-16, pp. 1–35, 2006.
- [13] W. Gautschi, "Leonhard euler: his life, the man, and his works," *SIAM review*, vol. 50, no. 1, pp. 3–33, 2008.
- [14] G. M. Hoffmann, H. Huang, S. L. Waslander, and C. J. Tomlin, "Quadrotor helicopter flight dynamics and control: Theory and experiment," in *Proc. of the AIAA Guidance, Navigation, and Control Conference*, vol. 2, 2007, p. 4.
- [15] J.-J. E. Slotine, W. Li *et al.*, *Applied nonlinear control*. Prentice hall Englewood Cliffs, NJ, 1991, vol. 199, no. 1.
- [16] *Pixhawk Pilot Support Package (PSP) User Guide, Version 2.0*. Pilot Engineering Group, The MathWorks, Inc., 2016.

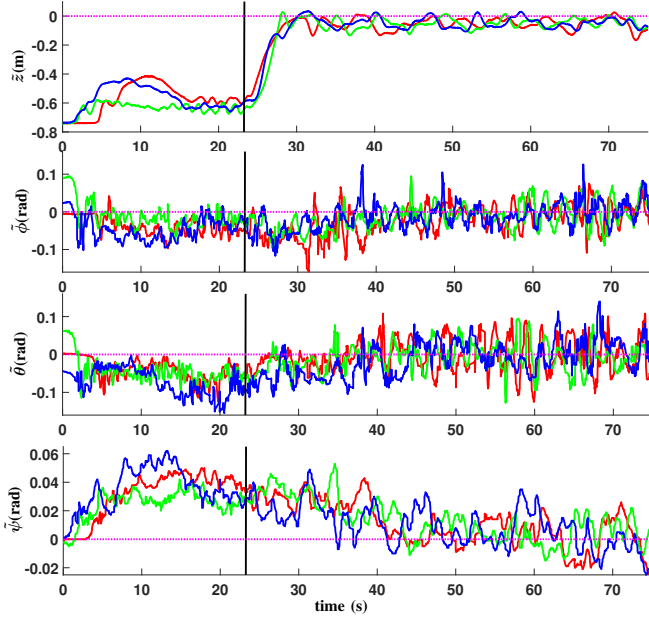


Fig. 7. Realtime observations of \tilde{z} , $\tilde{\phi}$, $\tilde{\theta}$ and $\tilde{\psi}$ in three experiments denoted by three different colors during a 75s long hovering flight, where the back solid lines are used to indicate the time when the adaptive control is activated.

and therefore have significantly different values of the torque parameter b_i . This was reflected in the resultant \hat{A} after the adaptive component had been activated for several seconds.

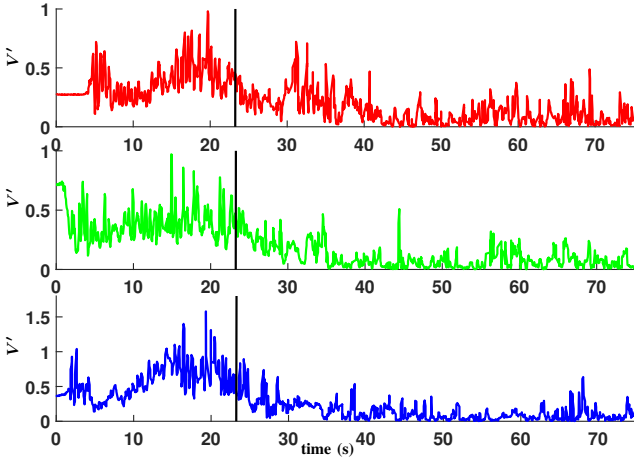


Fig. 8. Realtime partial Lyapunov function $V' = \frac{1}{2} s^T s$ in three experiments denoted by three different colors during a 75s long hovering flight, where the back solid lines are used to indicate the time when the adaptive control is activated.

Fig. 8 illustrates the realtime values of the partial Lyapunov function $V' = \frac{1}{2} s^T s$ before and after enabling the adaptive scheme was enabled (separated by black vertical lines) from three flights. Since we do not know the actual value of A , we can not calculate the \tilde{A} term in the original V . Three experimental results all prove that the value V' before enabling adaptive control is evidently larger than those after the adaptive scheme came into action, which evidently validates the performance of our proposed control strategy starting from an uncertain dynamic matrix.